

Equation (11) can be differentiated with respect to T to obtain $\Pi_1(E, T)$. We then find $\Pi_1(0, T) \propto T^2$ for $T \rightarrow 0$. Even though this $\Pi_1(E, T)$ is not analytic at $T = 0$ it may be substituted into Eq. (3) to yield

$$S(E, T)_{T \rightarrow 0} = (4kA_1/p)T^3 + \frac{1}{3}\beta T^3, \quad (13)$$

which is positive for $A_1 < p\beta/12k$. Certainly it is possible to have a nonanalytical form for $\Pi_1(E, T)$ which would have $\Pi_1(0, T) \propto T$ and still satisfy Eq. (3). However, excitation dispersion curves which are physically significant appear to rule out such a behavior. Because a negative Π_1 cannot be linear in T at low temperatures, electrocaloric cooling effects in lithium sulfate monohydrate below 1 K will be much smaller than predicted by Lang.⁶

Valuable discussions with Dr. R. L. Peterson and Dr. R. L. Kautz are gratefully acknowledged.

¹M. Born, *Rev. Mod. Phys.* **17**, 245 (1945).

²M. Born and K. Huang, *Dynamical Theory of Crystals* (Clarendon, Oxford, England, 1954), p. 327.

³P. J. Grout and N. H. March, *Phys. Rev. Lett.* **37**, 791 (1976), and *Phys. Rev. B* **14**, 4027 (1976), and *Phys. Lett.* **47A**, 288 (1974); P. J. Grout, N. H. March, and T. L. Thorp, *J. Phys. C* **8**, 2167 (1975).

⁴B. Szigeti, *Phys. Rev. Lett.* **37**, 792 (1976), and **35**, 1532 (1975).

⁵S. B. Lang, *Phys. Rev. B* **4**, 3603 (1971).

⁶S. B. Lang, *Ferroelectrics* **11**, 519 (1976). This article overlooks the negative sign in the pyroelectric coefficient at low temperatures.

⁷S. B. Lang, *Sourcebook of Pyroelectricity* (Gordon and Breach, New York, 1974), p. 23.

⁸M. E. Lines and A. M. Glass, *Phys. Rev. Lett.* **39**, 1362 (1977).

⁹R. Blinc and B. Zeks, *Soft Modes in Ferroelectrics and Antiferroelectrics* (North-Holland, Amsterdam, 1974).

¹⁰W. N. Lawless, *Phys. Rev. B* **14**, 134 (1976).

¹¹J. C. Holste and W. N. Lawless, *Bull. Am. Phys. Soc.* **19**, 649 (1974).

¹²J. D. Siegwarth and A. J. Morrow, *J. Appl. Phys.* **47**, 4784 (1976).

¹³D. H. Martin, *Magnetism in Solids* (MIT Press, Cambridge, Mass., 1967).

Work-Function Dependence of Negative-Ion Production during Sputtering

Ming L. Yu

Brookhaven National Laboratory, Upton, New York 11973

(Received 13 December 1977)

A systematic study was made of negative-ion formation by sputtering from a Mo(100) surface with and without adsorbate layers. Correlation with the work-function change when the surface electronic state was modified by a Cs overlayer reveals a possible tunneling mechanism. Tunnel barrier widths and heights were estimated for Mo^- , O^- , H^- , and D^- from the experimental data.

The formation of secondary ions during sputtering is the basis of secondary-ion mass spectrometry (SIMS). SIMS has rapidly become an important analytic technique especially for surface and metallurgical studies. Extremely high detection sensitivity for both elements and compounds has been achieved.¹ Quantitative application of SIMS, however, is unfortunately hindered by our lack of understanding of the secondary-ion formation process. In particular, there is still no microscopic description of negative SIMS. In this Letter, I report a systematic experimental study of the negative-ion formation process through its dependence on the work function of the specimen surface. An electron tunneling model has evolved from this work which can possibly form the basis for a microscopic theory of sec-

ondary ion formation.

The energy threshold of negative-ion formation is the difference between the surface work function and the electron affinity of the ion. A lower work function enhances the electron capture process as observed during sputtering with Cs^+ ions.^{2,3} I have looked into Mo^- formation⁴ from clean Mo(100) surfaces and the formation of H^- , D^- , $^{16}\text{O}^-$, and $^{18}\text{O}^-$ from adsorbed layers on Mo(100). In this experiment I deposited a submonolayer of Cs onto the sample surface to modify the surface work function. The secondary ion yields during low-energy Ne^+ bombardment were monitored as the work function changed with the Cs coverage. Some results with K overlayers are also presented.

The experiment was performed inside an ion-

pumped UHV system with a base pressure in the upper 10^{-11} range. High-purity single-crystal Mo(100) samples, 0.2 in. \times 0.5 in. \times 0.004 in. in size, were used. The crystal was oriented to better than 1° . The sample was resistively heated and the sample temperature was monitored with a W-26%Re-W-5%Re thermocouple. The sample cleaning procedure included heating the sample to 900°C in 10^{-6} Torr of O_2 for an hour to remove carbon, followed by flash heating to 1400°C to remove the oxygen. The sample was then examined (*in situ*) with an Auger-electron spectrometer to determine the surface cleanliness. The above procedure was repeated when necessary.

The primary ion beam used was a Ne^+ beam collimated to a beam diameter of 4 mm, with a 1-nA typical ion current. The incident angle was about 45° . During operation, the Ne partial pressure was in the 10^{-7} -Torr range in the chamber. A liquid-nitrogen-cooled Ti sublimation pump kept the other residual gases, mostly hydrogen, in the low 10^{-10} -Torr range. The Ne^+ current density was kept very low (< 10 nA/cm 2) to reduce the radiation damage on the sample surface. The total sputtering time in one run was typically 600 sec. Negative ions were detected by using a quadrupole mass spectrometer with the sample surface perpendicular to the mass spectrometer axis. The energy filter in front of the mass spectrometer had an energy passband roughly from 0 to 30 eV. No attempt was made at energy analysis of the secondary ions.

Cesium was applied to the sample surface by thermal evaporation from a thoroughly outgassed Cs getter.⁵ The rise in chamber pressure was less than 5×10^{-11} Torr during evaporation. Oxygen contamination, estimated to be about 5%, was observed in the Cs overlayer. The Cs coverage was increased in small steps while sputtering and negative-ion detection were done in between. The electron-beam retarding-potential method⁶ was used to measure the work-function change $\Delta\phi$ to an accuracy of about ± 0.05 V. Figure 1 shows the work-function change $\Delta\phi$ and the Mo^- yield as a function of Cs deposition time. The maximum work-function reduction was about 2.6 eV, in good agreement with the literature value. No Mo^- was detected above noise (~ 1 Hz) in the absence of Cs. With the gradual decrease in ϕ , the Mo^- yield increased rapidly and reached a maximum when $\Delta\phi$ was close to its minimum. The Mo^- yield dropped significantly as the Cs coverage increased further while ϕ rose to its

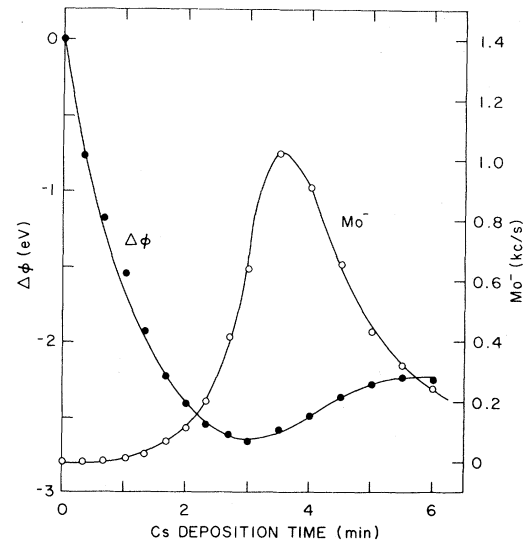


FIG. 1. Variation of ϕ and Mo^- yield with Cs deposition time. The Cs dependence of H^- , D^- , and O^- production was also very similar. The yield maxima correlate closely with the ϕ minima.

saturation value. The Cs dependence of H^- , D^- , and O^- production was also very similar. Some H^- data were reported previously.⁷ For H^- , the sample was exposed to 5×10^{-9} Torr of H_2 for 15 min, totaling an exposure of 4.5 L [1 L (Langmuir) = 10^{-6} Torr \cdot sec]. Work-function measurements showed a small (~ 0.1 eV) increase in ϕ resulting from the hydrogen overlayer. Then Cs was deposited onto this hydrogenated Mo surface and the experiment was repeated, as in the pure Mo case. The treatment with D_2 was exactly the same. Although both H^- and D^- yields had similar $\Delta\phi$ dependences, the D^- yield was usually an order of magnitude lower than that of H^- under similar experimental conditions.

For O^- , the clean Mo(100) surface was exposed to 1×10^{-8} Torr of $^{16}\text{O}_2$ or $^{18}\text{O}_2$ for 10 minutes, totaling an exposure of 6 L. The oxygen overlayer raised the work function by about 1.7 eV. Some evidence for patch formation was observed, but it rapidly went away with Cs deposition. The O^- yield was significantly enhanced by the deposition of Cs. However, the yield only decreased slightly with Cs coverage after reaching the maximum. ^{18}O was used to avoid complications from the oxygen contamination in the Cs overlayer. But no significant difference was noticed. The $^{18}\text{O}^-$ yield was usually 10 to 20% less than the $^{16}\text{O}^-$ yield under similar conditions. However, the oxygen contamination in the Cs prevented an accurate assessment of the effect of isotopic

mass differences.

When an atom escapes from a surface, it interacts with the surface electrons which leak into the vacuum. The tunneling of an electron between the escaping particle and the substrate can cause de-excitation, ionization, and neutralization.⁸⁻¹⁰ I found that my experimental data could readily be explained by a tunneling model. We represent the salient features of the tunneling process by two parameters: the height V_0 and the width a of the tunneling barrier. The electron tunneling probability is given by¹¹

$$p = \frac{16E(V_0 - E)}{V_0^2} \times \exp \left[-2 \left(\frac{2m}{\hbar^2} \right)^{1/2} (V_0 - E)^{1/2} a \right], \quad (1)$$

where E is the energy of the electron. None of the negative-ion yields monitored was proportional to the Cs coverage. This suggests that the ef-

fect of the Cs atoms was *nonlocal*. I shall postulate that the Cs overlayer changes the barrier height V_0 by $\Delta\phi$ so that

$$V_0 - E = V_1 + \Delta\phi, \quad (2)$$

where V_1 is the initial barrier height when there was no Cs. So the ion yield Y is related to the total sputtering yield Y_0 and the neutralization probability A of the ion by

$$Y = A Y_0 \frac{16E(V_1 + \Delta\phi)}{V_0^2} \times \exp \left[-2 \left(\frac{2m}{\hbar^2} \right)^{1/2} (V_1 + \Delta\phi)^{1/2} a \right]. \quad (3)$$

With the proper choices of V_1 and a , Eq. (3) fits the experimental data very well for a large Cs coverage range and over two orders of magnitude variation in yields, as shown in Fig. 2. By means of a least-squares fit, V_1 and a were determined for the various ion species and sputtering conditions. V_1 and a so determined have very reasonable physical values as shown in Table I. The least-squares fit was not very sensitive to the choice of V_1 since only the square root of the quantity $V_1 + \Delta\phi$ enters into the exponent. V_1 was only determined to ± 0.5 V.¹² Values of the barrier parameters determined for individual ion

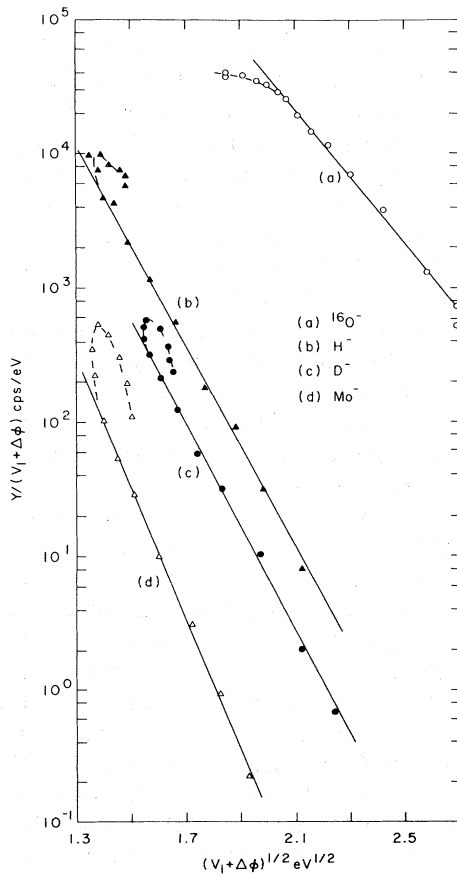


FIG. 2. Least-squares fit of the experimental data with the tunneling model. The values of V_1 and a are shown in Table I. The "loops" at high Cs coverages are still not understood.

TABLE I. V_1 , a , T_p , and T_p^* at different Ne^+ energies. The values of T_p^* calculated from V_1 and a as in the tunneling model agree very well with the values of T_p obtained by fitting with the LTE model.

Overlayer	Ion	Ne^+ energy (eV)	V_1 (eV)	a (Å)	T_p (K)	T_p^* (K)
Cs	Mo^-	500	4.5	10.97	3840	4380
		1500	4.5	10.37	4070	4630
		3500	5.0	10.57	4320	4790
	H^-	150	5.0	8.21	5630	6160
		500	4.5	7.96	5570	6030
		1500	5.5	8.16	6230	6500
	D^-	2000	5.0	7.60	6390	6660
		3500	5.5	7.78	6580	6820
		150	5.5	7.76	6590	6840
	$^{16}\text{O}^-$	500	5.0	8.67	5480	5840
		1500	5.0	8.33	5610	6080
		500	8.0	5.59	11060	11450
$^{18}\text{O}^-$	500	7.0	6.14	9320	9750	
	500	8.0	5.45	11690	11740	
	2500	7.5	5.59	10630	11090	
K	H^-	150	4.5	8.89	5020	5400
		500	4.5	8.86	5100	5420
		1500	4.5	8.65	5250	5550

species are consistent to within ± 0.5 eV and ± 0.5 Å of the averaged values of V_1 and a , respectively, in spite of over one order of magnitude change in the energy of the sputtering ions. Electronic excitations produced by the incident ions are expected to perturb these parameters. The data, however, seem to indicate that the effect is still small in this energy range. Although H^- and D^- showed very different yields, barrier parameters are practically unaffected by the isotopic mass difference. Using K instead of Cs for H^- production, however, gave a slightly larger barrier width. The evidence is that V_1 and a are probably related to the electronic transitions involved, and not the sputtering process. It also suggests that the large difference in the H^- and D^- yields is caused by a large difference either in the neutralization probabilities, similar to the isotope effect in electron-stimulated desorption,¹³ or in the sputtering coefficients between H^- and D^- , or both.

Deviations from Eq. (3) at zero and very high Cs coverages were observed. The negative-ion yields at zero Cs coverage were usually smaller than expected from Eq. (3). At high Cs coverages, the Mo^- , H^- , and D^- yields were higher while the O^- yield was lower than predicted. The reason is still not understood.

The most successful quantitative theory for SIMS is the local thermal equilibrium (LTE) theory² which assumes the formation of a local high-temperature plasma at the impact of an incident ion. The secondary ion yields are then determined by the Saga-Eggert equation which governs the equilibrium concentration of the secondary ions and electrons at the "plasma temperature" T_p . In LTE, the work-function dependence of the ion yield is

$$Y \propto \exp(-\Delta\phi/k_B T_p). \quad (4)$$

Although the LTE model is still the most useful theory available, there has been a lot of controversy over the physical significance of T_p . In practice, T_p is used as an experimental parameter and there is no theory of T_p .

In Eq. (3), the exponential function is the dominant term. For limited range of $\Delta\phi$, we can linearize the $\Delta\phi$ dependence in the argument:

$$Y \propto \exp[-2(2m/\hbar^2)^{1/2} V_1^{1/2} (1 + \Delta\phi/2V_1)a], \quad (5)$$

$$\propto \exp(-\Delta\phi/k_B T_p^*),$$

where

$$T_p^* = \frac{1}{k_B} \left(\frac{\hbar^2}{2m} \right)^{1/2} \frac{V_1^{1/2}}{a}. \quad (6)$$

Equation (5) is exactly the functional form expected from the LTE theory but with the "plasma temperature" T_p^* given by the microscopic quantities of the electronic transition and not by the sputtering parameters. Not surprisingly, my data fit Eq. (4) quite well except at zero and very high Cs coverages.⁷ The values of T_p obtained by a least-squares fit are shown in Table I. They agree very well with the values of T_p^* calculated from V_1 and a using Eq. (6). This analysis raises the question of whether the LTE expression is actually a restricted form of the tunneling equation (3), and whether its success is a consequence of the limited barrier-height variations in real systems.

The author would like to thank Dr. M. Strongin, Dr. T. Sluyters, and Dr. K. Prelec for useful discussions and Mr. G. Hrabak for his expert technical assistance. The research was supported by the U. S. Department of Energy.

¹H. W. Werner, *Surf. Sci.* **47**, 301 (1975).

²C. A. Anderson, *Int. J. Mass Spectrom. Ion Phys.* **2**, 61 (1969).

³P. Williams and C. A. Evans, Jr., *Appl. Phys. Lett.* **30**, 559 (1977).

⁴Here I refer to the most abundant isotope ⁹⁸Mo.

⁵SAES Getters, Buffalo, New York.

⁶D. L. Fehrs and R. E. Stickney, *Surf. Sci.* **8**, 267 (1967).

⁷M. L. Yu, in *Proceedings of the Symposium on Production and Neutralization of Negative Hydrogen Ions and Beams*, Brookhaven National Laboratory, Upton, New York, 1977 (to be published).

⁸H. D. Hagstrum, *Phys. Rev.* **96**, 336 (1954).

⁹W. F. Van Der Weg and P. K. Rol, *Nucl. Instrum. Methods* **38**, 274 (1965).

¹⁰J. R. Hiskes, A. Karo, and M. Gardner, *J. Appl. Phys.* **47**, 3888 (1976).

¹¹L. I. Schiff, *Quantum Mechanics* (McGraw-Hill, New York, 1968), 3rd Ed.

¹²A cross check was made by calculating the preexponential factor $164Y_0E/V_0^2$ which I estimated to have an upper limit of 10^{10} Hz/eV in my experiment.

¹³T. E. Madey and J. T. Yates, Jr., *J. Vac. Sci. Tech.* **8**, 525 (1971).